Simulation Research on the Quenching and Partition Process of a Medium Manganese Steel

X. M. Guo, X. L. Zhang, J. Y. Mao, and Z. J. Wang(✉)

School of Iron and Steel, Soochow University, Suzhou 215006, China
wangzijian@suda.edu.cn

Abstract. As a potential third-generation high-strength steel, the medium manganese steel has broad application prospects. Hot stamping technology can effectively solve the problems of large springback and large forming resistance in the cold stamping process of medium manganese steel. However, the hot stamped parts have low elongation, which cannot meet the crashworthiness requirements. The quenching-partition (QP) heat treatment process can greatly increase the elongation of the part without reducing or slightly reducing the material strength. The quenching temperature, partitioning temperature and partitioning time have a great influence on the microstructure and mechanical properties of the hot stamped part. In order to obtain the optimal process parameters, numerical simulation of the QP process based on three models were conducted. The results showed that the CCE model is simple to use but with large error. The results obtained from the carbon partition model considering interfacial migration agreed best with the experimental results.

Keywords: Q&P Process · CCE Model · Carbon Partition · Interface Migration

1 Introduction

As a potential third-generation high-strength steel, the medium manganese steel has broad application prospects [1–4]. Due to the high strength of medium manganese steel, it is easy to have problems such as large springback, poor dimensional accuracy and even cracking during traditional cold stamping [5]. At present, hot stamping is usually used [6, 7] to solve the problems. In order to improve the plasticity of hot formed parts, it is proposed to combine quenching and partition [7] (Q&P) process with hot stamping.

Speer JG [8] proposed a thermodynamic model: the limiting condition carbon balance model, also known as CCE model. However, in the later experiments, the obvious migration phenomenon of the interface between austenite and martensite was observed, and the driving force of the migration came from the difference of chemical potential on both sides of the interface. The movement of the interface will also have a great impact on the final content of retained austenite. Finally, based on the classical CCE model, two improved models are proposed: the CCE model considering carbon diffusion but no interface migration and the model considering carbon diffusion and interface migration.

Y. Zhang and M. Ma (Eds.): ICHSU 2022, AHMST 2, pp. 363–369, 2023.
https://doi.org/10.2991/978-94-6463-114-2_48

In this paper, a Fe-0.18C-4.76Mn-0.23Si steel was processed with Q&P process, three different thermodynamic mechanism models are used to simulate the Q&P process, in order to study the quenching-partition process under different process parameters (quenching temperature, partition temperature, partition time, etc.) and obtain the optimal process parameters.

2 Classical CCE Model

The volume fraction of martensite and austenite after quenching is obtained by K-M model, and the calculation formula is as follows:

$$f_M = 1 - \exp[\mathrm{a} \cdot (Ms - T)] \tag{1}$$

where f_M is the volume fraction of martensite; a is a constant, generally taken as 0.011; Ms is the starting temperature of martensite transformation, and T is the quenching temperature.

The martensite transformation starting temperature (Ms) is related to the composition of steel (wt.%), and the calculation formula is as follows:

$$Ms = 539 - 423C - 7.5Si - 30.4Mn - 17.1Ni - 12.1Cr - 7.5Mo + 30Al. \tag{2}$$

In the CEE model, it is assumed that the chemical potential of carbon at the interface is equal to (3); according to the Fe and C mass conservation Eqs. (4) and (5) in martensite and austenite after partition, and (6) according to the volume fraction of the two phases.

$$X^{\gamma}_{C-CCE} = X^{\alpha}_{C-CCE} \cdot \exp\{[76789 - 43.8T - (169105 - 1204T)X^{\gamma}_{C-CCE}]/RT\} \tag{3}$$

$$f^{\gamma}_{CCE}(1 - X^{\gamma}_{C_{CCE}}) = f_A(1 - X_C) \tag{4}$$

$$f^{\alpha}_{CCE}X^{\alpha}_{C-CCE} + f^{\gamma}_{CCE}X^{\gamma}_{C-CCE} = X_C \tag{5}$$

$$f^{\alpha}_{CCE} + f^{\gamma}_{CCE} = 1 \tag{6}$$

where X^{γ}_{C-CCE} and X^{α}_{C-CCE} are carbon concentrations in austenite and martensite after partitioning, respectively. f^{γ}_{CCE} and f^{α}_{CCE} are the volume fractions of austenite and martensite after partition respectively. f_A is the volume fraction of austenite before partitioning; X_C is the mole fraction of carbon.

Figure 1 shows the curve of the volume fraction of martensite and austenite before and after distribution with quenching temperature, which was calculated using the CCE model. With the increase of quenching temperature, the content of retained austenite first increases and then decreases. When the quenching temperature is 175 °C, the content of retained austenite reaches the maximum value of 20.87%, which is the best quenching temperature.

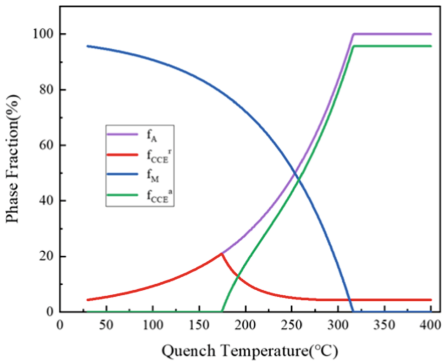

Fig. 1. Relationship between volume fraction of each phase and quenching temperature after Q&P treatment.

3 CCE Model Considering Diffusion but no Interface Migration

In the model without considering interface migration, there is only the process of carbon diffusion, which includes diffusion in austenite and martensite respectively and diffusion at martensite-austenite interface. The driving force of diffusion is the chemical potential difference of carbon, not the concentration difference. Therefore, although the concentration of carbon in martensite and austenite is equal after quenching, carbon will diffuse between austenite and martensite due to the difference of chemical potential between martensite and austenite after partition starts. The main basis of carbon diffusion in martensite and austenite is the solution of diffusion equation, which can be described by Fick's second law:

$$\frac{\partial x_C}{\partial t} = \frac{\partial}{\partial z}[\frac{D_C x_C}{RT}\frac{\partial \mu_C}{\partial z}] \tag{7}$$

In which x_C is carbon mole fraction, D_C is diffusion coefficient and μ_C is chemical potential.

In this model, the finite difference method is used to calculate the carbon diffusion in martensite and austenite. With the partition process, the carbon concentration in martensite and austenite changes constantly, and the chemical potential also changes accordingly. Through data fitting, the relationship between the chemical potential μ_C^α and μ_C^γ of carbon in martensite and austenite and the molar fraction x_C^α and x_C^γ can be obtained:

$$\mu_C^\alpha = 84273 + RT\ln(x_C^\alpha) + (1 - x_C^\alpha)^2(-18673) \tag{8}$$

$$\mu_C^\gamma = 77108 + RT\ln(x_C^\gamma) + (1 - x_C^\gamma)^2(-53699) \tag{9}$$

The program is compiled in Matlab to meet the above model conditions, the best quenching temperature calculated from CCE model is selected, and the partition temperature is 450 °C. Half of martensite size (400 nm) and half of austenite size (100 nm) are taken as calculation intervals, the interface width is 1nm, and the time step is 1 ×

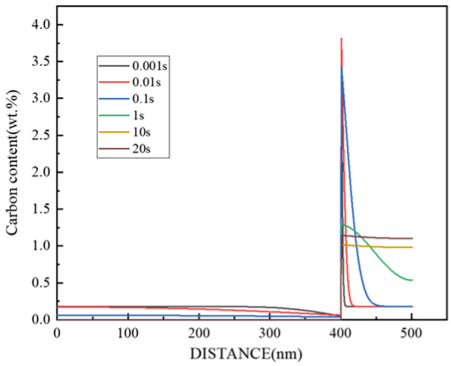

Fig. 2. Relationship between carbon content and composition time at 450 °C.

10^{-6} s. Figure 2 shows the simulation results of carbon content distribution in martensite and austenite regions when the partition time is 0.001 s, 0.01s, 0.1s, 1s, 10s and 20s, respectively. It can be seen from the figure that with a short distribution time (0.001 s, 0.01 s), carbon diffuses from martensite to austenite and accumulates at the austenite interface; With the prolongation of the partitioning time(0.1 s, 1 s), the carbon content at the austenite interface decreased and gradually diffused to the austenite center, resulting in a decrease in the overall carbon content of martensite and an increase in the overall carbon content of austenite; When the partition time increases to 10 s and 20 s, the carbon content in martensite and austenite reaches the equilibrium concentration and no longer changes, indicating that the whole partition process has been completed when the partition time is 10 s at 450 °C. At the end of the partition, the carbon content in the martensite reaches a very low value. During the whole partition process, the diffusion rate of carbon in martensite is significantly higher than that in austenite.

4 CCE Model Considering Diffusion and Interface Migration

Researchers observed obvious interface migration during Q&P process experiment. After that, Santofimia et al. Proposed a thermodynamic model considering carbon diffusion and interface migration. When there is a free energy difference on both sides of the interface, the interface will migrate. Because the carbon potential at the interface is equal, the driving force of interface migration is the chemical potential difference of iron atoms. The interface migration in the partition process, will have a certain impact on the content of residual austenite, and then affect the mechanical properties of Q&P steel.

In the thermodynamic model considering interface movement, it is necessary to consider the steps of carbon diffusion at the interface, interface movement, carbon diffusion at the interface during interface movement, and carbon diffusion in martensite and austenite. The carbon concentration at the interface between martensite and austenite is equal, and the carbon diffusion at the interface is the same as formula (3) in Sect. 2. The solution of carbon diffusion in martensite and austenite is also the same as that in

Sect. 3, which is solved by finite difference method. The calculation formula of interface moving speed is as follows:

$$v = (V_m)^{-1} \cdot M \cdot \Delta G = (V_m)^{-1} \cdot M \cdot k(x_c^{\gamma - eq} - x_c^{\gamma}) \tag{10}$$

where V_m is the molar volume of iron atom, M is the interface mobility, ΔG is the driving force, k is a constant, x_c^{γ} and $x_c^{\gamma - eq}$ are the carbon concentration and equilibrium carbon concentration of austenite at the interface, respectively.

When the interface moves, the solubility of carbon in austenite is much greater than that in martensite. In the process of interface movement, carbon diffuses from the moving interface to the untransformed austenite at the interface or from the untransformed martensite at the interface to the moving interface. The carbon diffusion at the interface can be calculated by the following formula:

$$J_m = v \cdot (c_{\text{int}}^{\gamma} - c_{\text{int}}^{\alpha}) \tag{11}$$

where v is the interface moving speed, and c_{int}^{r} a and c_{int}^{a} represent the molar volume concentration of carbon in austenite and martensite at the interface, respectively.

The model still takes Fe-0.18C-4.76Mn-0.23Si as the research object, and the data selection of quenching temperature, partition temperature, austenite and martensite size, and time step are consistent with the data in the previous chapter, which only considers carbon partition without considering interface movement. The model is simulated by finite difference method in Matlab.

Figure 3 is the simulation results of carbon content distribution in martensite and austenite regions under the model when the partition time is 0.001 s, 0.01 s, 0.1 s, 1 s, 10 s and 20 s respectively. It can be seen from the figure that when the partition time is short, the interface moves from austenite to martensite because the solubility of carbon in martensite is much smaller than that in austenite. At the beginning of the division, the carbon concentration of martensite is higher than the equilibrium concentration, and the carbon concentration of austenite is lower than the equilibrium concentration, so a large number of carbon atoms are diffused from martensite to austenite in a short time, and the diffusion rate of carbon in martensite is much higher than that in austenite, so the carbon concentration of austenite at the interface increases sharply. With the increase of the partition time, the carbon concentration in martensite gradually decreases. At this time, the carbon at the austenite interface moves to the low carbon position in the austenite, so that the carbon concentration at the interface decreases and the interface moves from martensite to austenite. As the interface moves, the volume fraction of martensite becomes higher and higher, and the carbon concentration in martensite decreases, while the carbon concentration in austenite increases gradually. When the carbon concentration of the two phases reaches their equilibrium carbon concentration, the partition process ends.

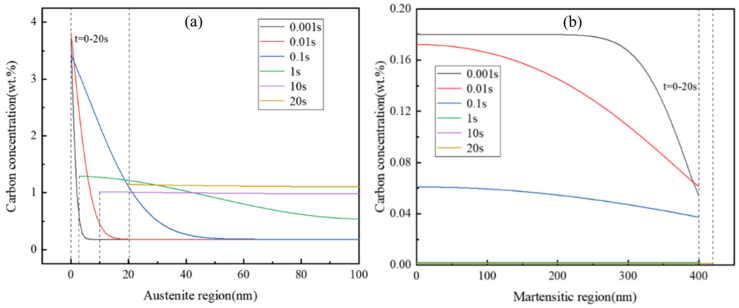

Fig. 3. (a) Carbon concentration distribution in the calculated region of austenite with different partition time; (b) Carbon concentration distribution in the calculated region of martensite with different partition time.

5 Conclusion

This paper mainly introduces the principles of the classical CCE model and two improved CCE models, in which the classical CCE model is the simplest, but the calculation formula of the classical CCE model has some errors, and the reliability of the calculation results is low. Although the calculation speed of the model considering only carbon diffusion is faster than that of the model considering carbon diffusion and interface migration, the results obtained are not reliable because the interface migration phenomenon is observed in the experiment and the interface migration is not considered in the model. The results obtained by the carbon partition model considering the interface migration are more consistent with the experimental results.

Acknowledgements. This research work was funded by the National Natural Science Foundation of China (Grant No. 51905189). The work was supported by the State Key Laboratory of Materials Processing and Die & Mould Technology, Huazhong University of Science and Technology [P2022–006].

References

1. Z. He, H. Yang, Y, He, W. Zheng and L. Li, Influence of manganese on deformation behavior of lightweight steel at different strain rate, *Journal of Materials Research and Technology* **9**, 11611 (2020).
2. A. S. Hamada, L. P. Karjalainen and M. C. Somani, The influence of aluminum on hot deformation behavior and tensile properties of high-Mn TWIP steels, *Materials Science & Engineering A* **467**, 114 (2007).
3. J. Galan, L. Samek and Verleysen, Advanced high strength steels for automotive industry, *Revista De Metalurgia* **48**, 118 (2012).
4. S. J. Lee, S. Lee and B. C. De Cooman, Mn Partitioning During the Intercritical Annealing of Ultrafine-Grained 6% Mn Transformation-Induced Plasticity Steel, *Scripta Materialia* **64**, 649 (2011).

5. H. Liu, X. W. Lu, X. J. Jin, D. Han and S. Jie, Enhanced Mechanical Properties of a Hot Stamped Advanced High-Strength Steel Treated by Quenching and Partitioning Process. *Scripta Materialia* **64**, 749 (2011).
6. B. Li and J. Z. Hong, The Research and Development of Hot Stamping Forming Technology and Production Line in View of High Strength Steel Plate, *Applied Mechanics and Materials* **2740**, 422 (2013).
7. J. G. Speer, D. V. Edmonds, F. C. Rizzo and D. K. Matlock, Partitioning of carbon from supersaturated plates of ferrite, with application to steel processing and fundamentals of the bainite transformation, *Current Opinion in Solid State & Materials Science* **8**, 219 (2004).
8. J. Speer, D. K. Matlock, B. C. De Cooman and J. G. Schroth, Carbon partitioning into austenite after martensite transformation, *Acta Materialia* **51,** 2611 (2003).